

Enhanced coupling to vertical radiation using a two-dimensional photonic crystal in a semiconductor light-emitting diode

Alexei A. Erchak,^{a)} Daniel J. Ripin, Shanhui Fan, Peter Rakich, John D. Joannopoulos, Erich P. Ippen, Gale S. Petrich and Leslie A. Kolodziejski
Research Laboratory of Electronics and Center for Materials Science and Engineering, Massachusetts Institute of Technology, Cambridge, Massachusetts 02139-4307

(Received 24 August 2000; accepted for publication 27 November 2000)

Enhanced coupling to vertical radiation is obtained from a light-emitting diode using a two-dimensional photonic crystal that lies entirely inside the upper cladding layer of an asymmetric quantum well structure. A sixfold enhancement in light extraction in the vertical direction is obtained without the photonic crystal penetrating the active material. The photonic crystal is also used to couple pump light at normal incidence into the structure, providing strong optical excitation.

© 2001 American Institute of Physics. [DOI: 10.1063/1.1342048]

Semiconductor light-emitting diodes (LEDs) have the potential to be low-cost and long lifetime solid-state lighting sources for applications as varied as room lighting to flat-panel displays.¹⁻³ LEDs are also used in short-range telecommunication systems and may be desirable for optical interconnects in computers.^{4,5} Unfortunately, most of the light emitted from a semiconductor LED is lost to guided modes within the high dielectric material, resulting in a low extraction efficiency. Here, two-dimensional (2D) photonic crystals are utilized to (1) enhance extraction of light in the vertical direction from a LED and (2) directly couple light from a pump laser into the LED structure, providing enhanced optical pumping. In contrast to previous work,^{6,7} no active material is removed to form the photonic crystal.

A 2D photonic crystal consisting of a triangular lattice of holes is etched into the upper cladding layer of an asymmetric LED structure that emits 980 nm light. The structure (Fig. 1) consists of an InGaP/InGaAs active region on top of a low dielectric Al_xO_y spacer layer and an Al_xO_y/GaAs distributed Bragg reflector (DBR). The asymmetric active region consists of 32 nm of InGaP beneath an 8 nm InGaAs quantum well (QW); the upper InGaP has a thickness of either 95 nm or 158 nm. The QW photoluminescence (PL) spectrum exhibits a full width at half maximum (FWHM) of ~65 nm at room temperature. To minimize nonradiative carrier recombination at the air hole surfaces, and to retain all of the active material in the structure, the holes do not penetrate the InGaAs QW. The asymmetry of the active region, however, allows the etched holes of the photonic crystal to be deep enough to cause strong Bragg scattering of the index-guided light. The DBR stop band ranges from 800 to 1300 nm and reflects the QW emission. The 0.5 μm low dielectric Al_xO_y layer minimizes the coupling to the lateral guided modes in the high-dielectric layers of the DBR. A 30 μm × 30 μm photonic crystal region is centered within a 50 μm or a 100 μm square LED mesa.

The LED structure is grown on (001) GaAs using gas-source molecular beam epitaxy. The Al_xO_y layers are initially grown as AlAs in the DBR and AlGaAs in the spacer

layer. The photonic crystal region is patterned using electron beam lithography; the pattern is transferred into the upper InGaP layer by reactive-ion etching (RIE) in a CH₄:H₂ plasma using a SiO₂ hard mask. Square mesas are defined using contact photolithography; RIE with a BCl₃:Cl₂:He plasma forms the LED mesa. Finally, the AlGaAs and the AlAs are thermally oxidized from the edge of the mesa.

In a semiconductor slab without a photonic crystal, ~1/(4n²) of the light emitted from the QW radiates through the top and bottom, where *n* is the index of refraction; photon recycling increases this estimate slightly.⁸ The DBR reflects the downward propagating light so that ~1/(2n²) of the emitted light radiates through the top surface. For the active region, *n* ≈ 3.2 so that only about 5% of the emitted light emerges from the top surface (without the photonic crystal). The rest of the emitted light lies below the light line of air, defined as $\omega = c|\mathbf{k}_0|$, where \mathbf{k}_0 is the in-plane wave vector in air (parallel to the surface of the LED structure). Modes below the light line ($|\mathbf{k}| > |\mathbf{k}_0|$), where \mathbf{k} is the in-plane wave vector of the emitted light propagating in the active region, suffer total internal reflection at the air/semiconductor interface and cannot phase match to the radiation modes ($|\mathbf{k}| < |\mathbf{k}_0|$). The photonic crystal, however, folds the guided modes at the Brillouin zone boundaries, allowing phase matching to the radiation modes that lie above the air light line.⁹ Phase matching requires that $\mathbf{k}_0 = \mathbf{k} \pm \mathbf{G}$, where \mathbf{G} is a reciprocal lattice vector of the photonic crystal. The guided modes that phase match to radiation modes become leaky resonances of the photonic crystal. Thus, the photonic crystal Bragg scatters emitted light out of the active region, leading to higher extraction efficiencies.¹⁰ Similarly, without the photonic crystal, incident pump light that lies above the light line does not couple into guided lateral modes of the semiconductor slab. Instead, the pump light is reflected or transmitted and does not propagate in the semiconductor slab where it can be readily absorbed by the QW. Pump light incident on the photonic crystal may also phase match to resonant modes, providing a pathway for strong optical pumping of the QW.

Coupling to an optical fiber requires efficient extraction from the LED, specifically in the vertical direction.^{11,12} Ver-

^{a)}Electronic mail: aacherchak@mit.edu

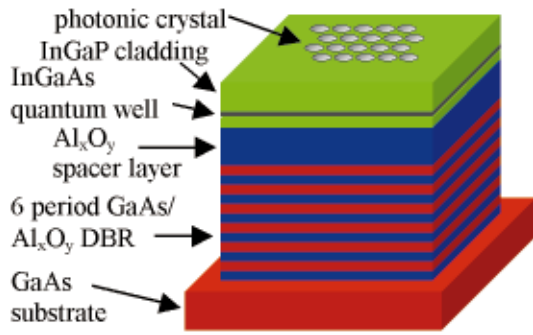


FIG. 1. (Color) LED mesa containing a triangular photonic crystal (schematic).

tical radiation ($\mathbf{k}_0=0$) only couples to modes with zero in-plane wave vector plotted at the Γ point on a photonic band diagram. A resonance is created in the photonic crystal at the Γ point when multiple plane waves ($\mathbf{k}=\pm\mathbf{G}$) counterpropagate along directions of high symmetry so that their wave

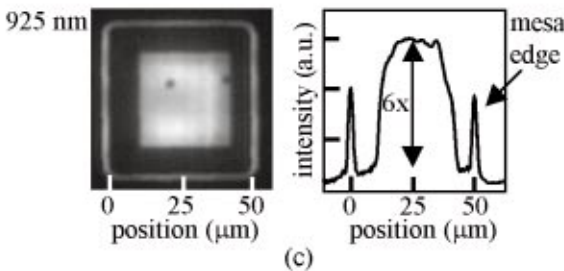
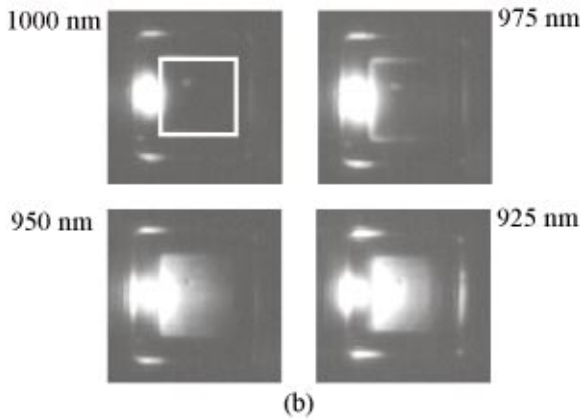
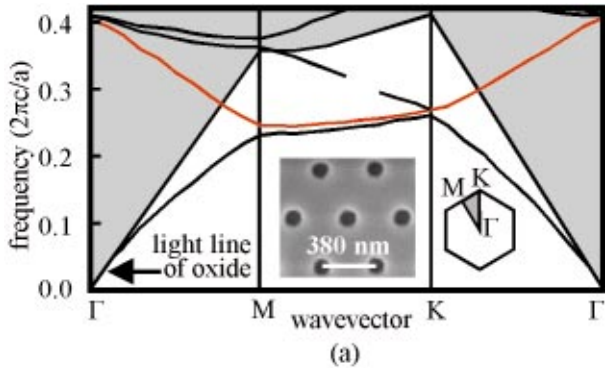


FIG. 2. (Color) (a) The calculated photonic band diagram for a triangular photonic crystal that enhances the extraction of light from the LED. In the inset is the SEM of the photonic crystal along with the first Brillouin zone. (b) CCD images of a photonic crystal centered within a LED mesa at various wavelengths. (c) Sixfold intensity enhancement near $\lambda=925$ nm.

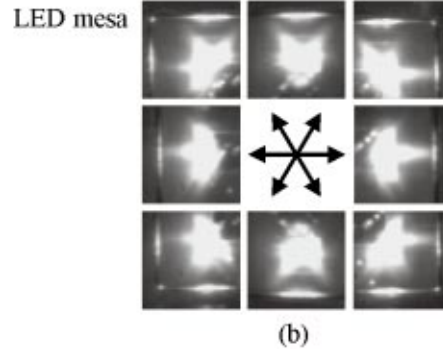
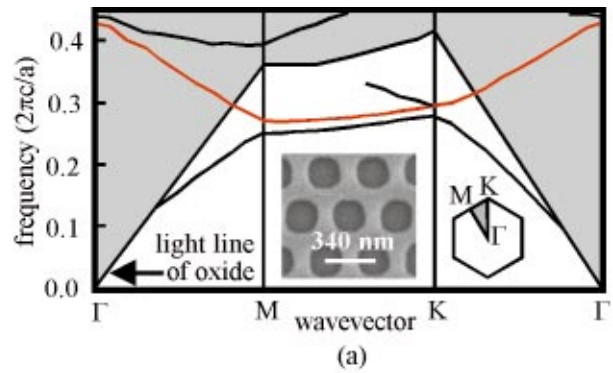


FIG. 3. (Color) (a) Calculated photonic band diagram for a triangular photonic crystal that enhances the optical pumping of the LED. In the inset is the SEM of the photonic crystal along with the first Brillouin zone. (b) Composite of CCD images detecting the entire InGaAs QW spectrum.

vectors form a standing wave pattern. The dimensions of the photonic crystal and the total thickness of the active region determine the wavelength of the resonance at the Γ point. A calculated photonic band diagram for a triangular photonic crystal with a lattice constant, $a=380$ nm, hole radius, $r=56$ nm, and hole depth, $d=101$ nm, having a 198 nm thick active region, is shown in Fig. 2(a). A scanning electron micrograph (SEM) of the photonic crystal is shown in the inset. A three-dimensional band structure calculation is performed using a conjugate gradient plane-wave expansion method¹³ in which the active region is on top of a semi-infinite oxide layer and below a semi-infinite air region. The QW primarily emits radiation with a transverse electric (TE) field polarization. The LED structure is asymmetric, however, so that the modes plotted are not strictly TE, but still maintain at least 80% of the electric field polarized in the plane of the active region.¹⁴ Above the light line, only optical modes with at least 80% of the electric field intensity concentrated in the active region are plotted. A clear folding of

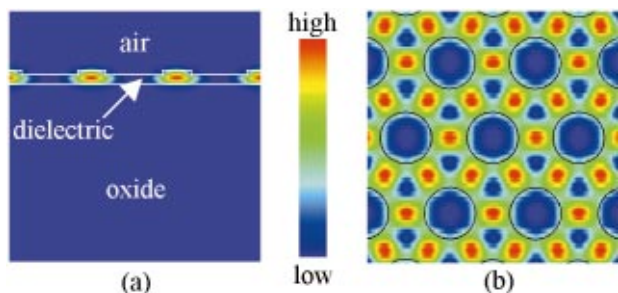


FIG. 4. (Color) Electric field intensity at resonance (790 nm) for the 2D photonic crystal LED structure. (a) Side view. (b) Top view.

guided modes below the light line (white region) occurs at the high symmetry boundary points of the first Brillouin zone (inset). A band is created (plotted in red) that extends above the light line (shaded region) and intersects the Γ point at a frequency of $0.4064 (2\pi c/a)$, which corresponds to 935 nm.

Spatial and spectral charge coupled device (CCD) images of room temperature PL are used to characterize a LED mesa containing a photonic crystal. The PL is excited with a continuous wave (cw) Ti:Al₂O₃ laser pumping at 810 nm. The pump beam, which is focused to a $<5 \mu\text{m}$ spot size on the sample, is absorbed by the InGaAs QW layer and not by the InGaP cladding layers, and it is reflected by the underlying DBR. The focusing lens collects light up to 15° off axis with the normal direction. CCD images of a LED mesa containing the photonic crystal featured in Fig. 2(a) are taken with four different optical filters [Fig. 2(b)]. Each filter transmits a spectral range of 10 nm FWHM centered about 925, 950, 975, and 1000 nm. By optically pumping a region outside the photonic crystal (outlined with a white square), light that is emitted from the QW is index guided in all lateral directions, with some of the light coupling to modes in the photonic crystal. Only wavelengths of the QW emission near the calculated 935 nm resonance at the Γ point are efficiently extracted in the vertical direction. Therefore, the image taken at 925 nm shows high light extraction while the 950 nm image shows less light being extracted. CCD images taken at 975 and 1000 nm exhibit poor light extraction since they are too far from the resonance at the Γ point. By optically pumping the entire mesa, the average PL intensity within the photonic crystal is plotted as a function of position [Fig. 2(c)]. The PL intensity near $\lambda=925$ nm emitted from the region without the photonic crystal is strongest in the vertical direction, yet is six times less than the intensity observed from the region with the photonic crystal.

Coupling the 810 nm pump light into the LED structure to enhance optical pumping requires a triangular photonic crystal with a smaller effective index than the photonic crystal used to enhance extraction; this is accomplished by using a larger hole diameter, a smaller lattice constant, and holes etched deeper with respect to a thinner active region. Figure 3(a) shows the photonic band diagram for such a triangular photonic crystal with $a=340$ nm, $r=104$ nm, and $d=60$ nm, having a 135 nm thick active region. A SEM of the photonic crystal is shown in the inset. The optical modes plotted are TE like and satisfy the same criteria as the modes plotted in Fig. 2(a). A resonance at the Γ point is calculated to be near $0.4304 (2\pi c/a)$, which corresponds to 790 nm. Figure 3(b) shows a composite image of eight CCD images taken with a broad spectral filter that covers the entire QW emission spectrum. For each image, the pump light is focused down to a $<5 \mu\text{m}$ spot size and excites a region inside the edge of the photonic crystal featured in Fig. 3(a). Enhanced optical pumping is observed outside the photonic crystal region along the six equivalent ΓM directions of the

triangular photonic crystal, indicating an apparent strong coupling to the resonance at the Γ point. The collection angle of the focusing lens combined with inaccuracies of the SEM micrographs ($\sim \pm 5$ nm) give some spread to the resonance at Γ .

The electric field intensity inside the LED structure for the resonant mode at 790 nm at the Γ point is determined from the band structure calculation for the photonic crystal [Fig. 3(a)] and is shown in Fig. 4. More than 99% of the electric field intensity is concentrated in the dielectric region (side view), giving further evidence of the true waveguiding nature of the resonance at the Γ point. The symmetry of the optical mode is due to the overlap of six plane waves propagating in each of the equivalent ΓM directions (top view). Since most of the electric field intensity is concentrated in the dielectric, the effective index inside the photonic crystal region for the resonant mode matches well with the slab region outside the photonic crystal. As a result, refraction at the interface between the photonic crystal and the slab region is low and the pump light emerges from the photonic crystal region along the ΓM directions, in agreement with the CCD images [Fig. 3(b)].

In summary, coupling between vertical radiation modes and a leaky resonant mode was presented using a 2D photonic crystal within the upper cladding layer of an asymmetric LED structure. A sixfold PL intensity enhancement near $\lambda=925$ nm was obtained. Input coupling of the 810 nm pump light was achieved, providing enhanced optical pumping. The enhancements are achieved without the photonic crystal penetrating the QW.

The authors would like to acknowledge Professor Henry I. Smith and Mark Mondol for their contributions. This work was supported by the NSF (Grant No. DMR-9808941).

- ¹M. G. Craford, IEEE Circuits Devices Mag. **8**, 24 (1992).
- ²I. Schintzer, E. Yablonovitch, C. Caneau, T. J. Gmitter, and A. Scherer, Appl. Phys. Lett. **63**, 2174 (1993).
- ³H. Benisty, H. De Neve, and C. Weisbuch, IEEE J. Quantum Electron. **34**, 1612 (1998).
- ⁴E. A. Fitzgerald and L. C. Kimerling, MRS Bull. **23**, 39 (1998).
- ⁵A. Forchel and P. Malinverni, Compd. Semicond. **6**, 74 (2000).
- ⁶M. Boroditsky, R. Vrijen, T. F. Krauss, R. Coccioli, R. Bhat, and E. Yablonovitch, J. Lightwave Technol. **17**, 2096 (1999).
- ⁷M. Boroditsky, T. F. Krauss, R. Coccioli, R. Vrijen, R. Bhat, and E. Yablonovitch, Appl. Phys. Lett. **75**, 1036 (1999).
- ⁸M. Boroditsky and E. Yablonovitch, Proc. SPIE **3002**, 119 (1997).
- ⁹V. N. Astratov, I. S. Culshaw, R. M. Stevenson, D. M. Whittaker, M. S. Skolnick, T. F. Krauss, and R. M. De La Rue, J. Lightwave Technol. **17**, 2050 (1999).
- ¹⁰S. Fan, P. R. Villeneuve, J. D. Joannopoulos, and E. F. Schubert, Phys. Rev. Lett. **78**, 3294 (1997).
- ¹¹A. Mekis, A. Dodabalapur, R. E. Slusher, and J. D. Joannopoulos, Opt. Lett. **25**, 942 (2000).
- ¹²M. Imada, S. Noda, A. Chutinan, T. Tokuda, M. Murata, and G. Sasaki, Appl. Phys. Lett. **75**, 316 (1999).
- ¹³R. D. Meade, A. M. Rappe, K. D. Brommer, and J. D. Joannopoulos, Phys. Rev. B **48**, 8434 (1993).
- ¹⁴S. G. Johnson, S. H. Fan, P. R. Villeneuve, J. D. Joannopoulos, and L. A. Kolodziejcki, Phys. Rev. B **60**, 5751 (1999).